analytical chemistry

pubs.acs.org/ac Article

Acoustic Methodology for Selecting Highly Dissipative Probes for Ultrasensitive DNA Detection

Dimitra Milioni,[§] Pablo Mateos-Gil,[§] George Papadakis, Achilleas Tsortos, Olga Sarlidou, and Electra Gizeli*

Cite This: *Anal. Chem.* 2020, 92, 8186–8193 Read Online

ACCESS | Metrics & More | Article Recommendations | Supporting Information

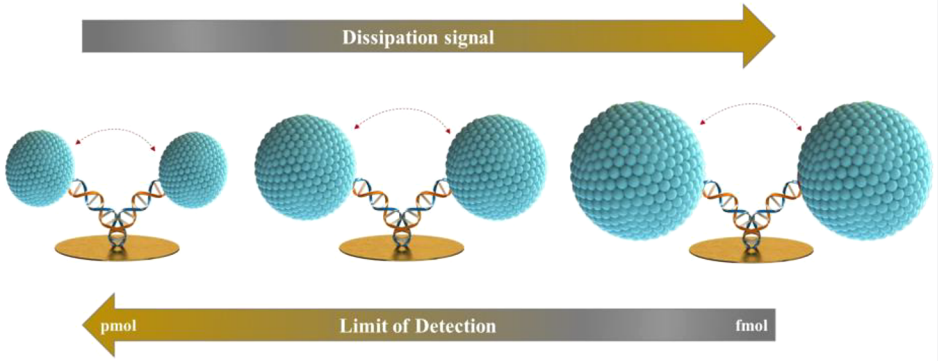

ABSTRACT: The objective of this work is to present a methodology for the selection of nanoparticles such as liposomes to be used as acoustic probes for the detection of very low concentrations of DNA. Liposomes, applied in the past as mass amplifiers and detected through frequency measurement, are employed in the current work as probes for energy-dissipation enhancement. Because the dissipation signal is related to the structure of the sensed nanoentity, a systematic investigation of the geometrical features of the liposome/DNA complex was carried out. We introduce the parameter of dissipation capacity by which several sizes of liposome and DNA structures were compared with respect to their ability to dissipate acoustic energy at the level of a single molecule/particle. Optimized 200 nm liposomes anchored to a dsDNA chain led to an improvement of the limit of detection (LoD) by 3 orders of magnitude when compared to direct DNA detection, with the new LoD being 1.2 fmol (or 26 fg/μL or 2 pM). Dissipation monitoring was also shown to be 8 times more sensitive than the corresponding frequency response. The high versatility of this new methodology is demonstrated in the detection of genetic biomarkers down to 1−2 target copies in real samples such as blood. This study offers new prospects in acoustic detection with potential use in real-world diagnostics.

Current trends in diagnostics stress the need for developing highly sensitive methods for nucleic acids detection, ideally without the need for extensive sample pretreatment and/or lengthy amplification procedures. The polymerase chain reaction (PCR), currently the ultimate in terms of sensitivity, has significant drawbacks, namely, high complexity, sensitivity to contamination, cost, lack of portability, and bias toward some specific sequences;[1] thus, the use of alternative means to reduce the number of steps or even eliminate completely the need for enzymatically amplified DNA targets is highly desirable.[2,3] Toward this end, the use of biosensors combined with sensitive signal enhancers has been extensively exploited to develop rapid nucleic acid detection methods leading to novel and improved transduction processes.[4] Nanotechnology and the development of novel materials have played a significant role in producing probes for signal amplification. Nanoparticles (NPs) of various compositions and structures and with unique and tunable electrical, magnetic, or optical properties have been used extensively for biomolecular recognition and molecular diagnostics for the detection of genetic biomarkers.[1,5−8] Nanoparticles typically functionalized with a specific nucleic acid probe bind with high selectivity and specificity to the surface of an appropriate transducer in the presence of the complementary target analyte.[6,7] Surface plasmon resonance-based works using NPs have led to ultrasensitive DNA detection (pM−fM),[1,7,9−11] especially when coupled with multiple NPs (zM).[12] In the case of electrochemical sensors, Au NPs have also served as signal amplifiers of the electrical impedance and capacitance signals as well as redox-active probes through various assay formats,

Received: January 24, 2020
Accepted: May 25, 2020
Published: May 25, 2020

https://dx.doi.org/10.1021/acs.analchem.0c00366
Anal. Chem. 2020, 92, 8186−8193

with reported detection limits in the fM and sub-fM range[1,6,7,10,13] or even lower ones (aM) in the case of a dual amplification and multifunctional Au NPs.[14]

Acoustic wave or piezoelectric devices are also well-suited to be combined with nanoparticles for improved signal response. In early studies, a quartz crystal microbalance (QCM) was used with single or multiple liposome probes per DNA target in a typical sandwich assay with a detection limit in the pM[15] and fM[15−19] ranges, respectively. The catalytic deposition of Au on already immobilized Au probes has also been used for ultrasensitive DNA acoustic detection.[20] In these examples, the added mass of the bound NP and the well-known mass-sensing approach, monitored through frequency change (ΔF), were exploited.

In the current work, we are presenting a new concept for acoustic signal amplification based on the use of soft liposomes and their ability to dissipate acoustic energy. Recently, energy losses measured through the change in the dissipation (ΔD) alone, or in combination with a corresponding frequency change (ΔF) in the form of the acoustic ratio ($\Delta D/\Delta F$), have been used as an alternative means to biosensing providing unique information. This new information concerns the size of solid nanoparticles deposited on the surface as a film;[21] the size, thickness, and/or stiffness of liposomes adsorbed on the device;[22,23] the conformation of suspended DNA or streptavidin molecules;[24−27] and conformational changes of biomolecules upon exposure to a specific ligand.[28−32] The proposed mechanism of the observed dissipation change is based on hydrodynamic acoustic coupling for both suspended molecules[25−27,33] and surface-adsorbed nanoentities.[22,23,34,35] The central aim of our study is to exploit hydrodynamic acoustic sensing by designing and selecting nanoentities that exhibit an enhanced dissipation response upon surface binding. We propose a new type of acoustically "lossy" nanoprobes, optimized on the basis of their geometrical features. Liposomes of a specific size were used for the ultrasensitive detection of DNA. We further employed the derived protocols for the detection of low amounts of DNA targets and a single nucleotide polymorphism (SNP) in crude human samples. To our knowledge, this is the first time where acoustic signal enhancement is based on dissipation measurements and highly dissipative acoustic probes.

Concept of Dissipation Capacity. Surface-attached biomolecules in a suspended way dissipate acoustic energy during oscillation in the low-MHz frequency range (5−150 MHz) as a result of, among other things, hydrodynamic effects. Fluid drag exerted on the bound nanoentity, together with flow distortion, results in mechanical stress exerted on the device surface. One of the consequences of molecular hydrodynamic sensing is that biomolecules with the same molecular "dry" mass may differ substantially in their ability to dissipate energy if their hydrodynamic volume or conformation differs (Figure 1A). This concept opens up the possibility to design ultrasensitive acoustic signal "amplifiers" by optimizing their shape and size rather than their mass. Despite considerable progress made in the field, the exact mechanism of energy losses occurring on the device surface is still a subject of intense investigation;[35] for this reason, an experimental approach is proposed in order to provide a measure for comparing the relative biomolecules' and nanoparticles' ability to dissipate acoustic energy. Previous studies from our group[32] as well as others[21,23,35] have shown that the measured dissipated energy per unit mass, i.e., the acoustic ratio of

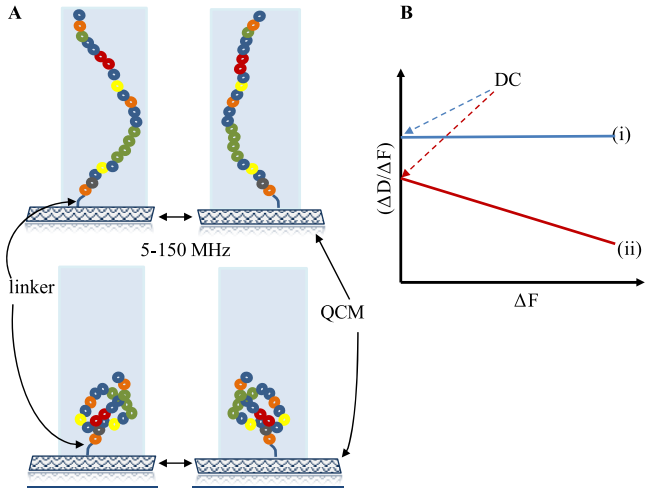

Figure 1. (A) Schematic representation of two biomolecules suspended on the oscillating QCM-D device surface via a single attachment point; note that the "dry" mass of the two molecules is kept the same while the shape is modified. (B) Curves reported in the literature depicting the dependency of the acoustic ratio ($\Delta D/\Delta F$) of an attached nanoentity on the surface mass density (ΔF): type (i) curve is obtained during the binding of DNA molecules[26,36] and streptavidin[24] through a single point, and type (ii) has been reported for proteins and liposomes adsorbed directly to the surface[23,37] or a protein suspended on a supported lipid bilayer.[32] The graphical definition of the DC value in the $\Delta D/\Delta F$ versus ΔF plot is also shown.

$\Delta D/\Delta F$, may depend on the amount of surface loading (Figure 1B). This observation makes the expression of acoustic ratio inadequate for comparing different biomolecules because in some cases the exact loading should also be reported. To fill this gap, we introduce the dissipation capacity (DC) of a surface-bound entity, defined as

$$\mathrm{DC} = \lim_{\Delta F \to 0} (\Delta D/\Delta F) \ (\text{in units of } 10^{-6}/\mathrm{Hz}) \quad (1)$$

which represents acoustic-energy dissipation of a single-molecule or nanoparticle.[32] Note that in the above expression ΔF is considered as directly related to the number of entities attached to the device surface. The aim of this approach is to select the most dissipative nanoentity based on its DC value and subsequently use it for effective dissipation amplification and ultrasensitive DNA detection. Moreover, we are interested in using these findings to understand the underlying biomolecular properties and mechanisms that govern acoustic-energy dissipation in order to be able to rationalize and control this process.

EXPERIMENTAL SECTION

Materials. Analytical-grade chemicals were purchased from Sigma-Aldrich. Lipid 1-palmitoyl-2-oleoyl-*sn*-glycero-3-phosphocholine (POPC) was purchased from Avanti Polar Lipids (Alabaster, AL, U.S.A.). Neutravidin was purchased from Invitrogen or Thermo Fisher.

Preparation of dsDNA Fragments. All high-performance liquid chromatography (HPLC)-grade DNA nucleotides were purchased from Metabion GmbH (Germany) except for the double-labeled (biotin and cholesterol) 50 nt purchased from Eurogentec S.A. (Belgium).

Oligonucleotides were dissolved in miliQ water (100 μM) and stored at −20 °C. To produce the 21, 50, and 75 bp

https://dx.doi.org/10.1021/acs.analchem.0c00366
Anal. Chem. 2020, 92, 8186−8193

dsDNA fragments, the double-labeled and corresponding complementary strands shown in Table S1 were mixed in a molar ratio of 1:10 (DNA concentrations of 1 and 10 μM, respectively) in 100 μL of phosphate-buffered saline (PBS); the solution was heated at 95 °C for 5 min for DNA strand denaturation and left for 1 h at room temperature (RT) to hybridize. Stock solutions of dsDNA fragments were stored at −20 °C and used within 1 month and up to 10 freeze/thaw cycles.

Liposome Preparation. Lyophilized lipids were dissolved in chloroform, dried under N_2, and resuspended at a final concentration of 2 mg/mL in PBS after gentle vortexing. The resulting suspension was passed through polycarbonate membranes (Whatman Nucleopore) with nominal pore diameters of 30, 50, 100, and 200 nm using the Avanti Mini-Extruder. Stock solutions were stored at 4 °C and used within 3 days. The extrusion method for liposome preparation results in rather narrow size distributions, as measured by light scattering, with average diameters near those of the filter pore.[38−40] Zeta potential measurements have shown that POPC particles carry zero charge ($\zeta \approx -2$ mV) when the buffer has a pH of ∼7.4 and the NaCl concentration is 150 mM.[39]

Quartz Crystal Microbalance with Dissipation Monitoring. A quartz crystal microbalance with dissipation monitoring (QCM-D) (Q-Sense E4, Biolin Scientific, Sweden) was used. Measurements were performed with a continuous flow rate of 60 μL/min and at 25 °C. The reported values of ΔF and energy dissipation ΔD were obtained at 35 MHz (7th overtone); ΔF was not normalized by the overtone number. Before use, the gold-coated crystals (Q-Sense QSX 301) were cleaned with Hellmanex 2%, rinsed with mili-Q water, dried under N_2, and treated for 30 min with UV/ozone (Ossila, Ltd., Sheffield).

Ultrasensitive Detection of DNA Molecules. The injection of 600 μL of low concentrations of DNA (from 1 pM to 2 nM) was followed by the addition of 600 μL of 0.2 mg/mL solution of 50 nm or 200 nm POPC liposomes.

Detection of DNA Targets in Molecular Diagnostics. DNA amplicons of 157 bp DNA were produced by PCR using a biotinylated forward primer (5′-biotin-tcctgatgggttgtgtttgg-3′) and a cholesterol-modified reverse primer (5′-cholesterol-tggtggggtgagatttttgtc-3′) (Eurogentec, Belgium). Five pmol of each primer was mixed with KAPA 2G Hot Start mix (KAPABIOSYSTEMS) in 10 μL final volume; 500 pg of a 249 bp DNA fragment containing the sequence of interest (BRCA1/Exon 20:1548-1797) was added as a template. The cycling protocol consisted of 5−30 cycles at 95 °C for 10 s, 62.5 °C for 10 s, and 72 °C for 10 s. An initial denaturation step for 5 min at 95 °C and a final extension step at 72 °C for 1 min were included in the amplification protocol.

Whole blood PCR was performed with KAPA Blood polymerase kit (Kapa Biosystems) using 2.5 μL of K_2EDTA and whole blood from a healthy donor (kindly provided by the University Hospital of Heraklion) in a total volume of 25 μL. Whole blood was first incubated for 10 min at RT with 0.1% Triton X-100 and then added in the PCR mix. PCR amplicons of 194 bp were produced using 5 pmol of a biotinylated forward primer (5′-gctccacttccattgaaggaagc-3′) and 30 pmol of a cholesterol-modified reverse primer (5′-cholesterol-tggtggggtgagatttttgtc-3′). The cycling protocol consisted of 35 cycles at three different temperatures: 95 °C for 30 s, 55 °C for 30 s, and 72 °C for 10 s. An initial denaturation step for 10 min at 95 °C and a final extension step at 72 °C for 10 min were included in the amplification protocol. BseRI restriction endonuclease (0.5 μL) (NEB, U.S.A.) was used to digest 12.5 μL of whole blood PCR reactions including 1.5 μL of 10× NEB buffer 4 at 37 °C for 1 h.

RESULTS AND DISCUSSION

The QCM-D device was used in all experiments to measure the acoustic ratios and derive the corresponding DC values of DNA molecules and DNA/liposome complexes. Liposomes were chosen as soft nanoprobes because in previous studies it has been shown that a large dissipation response was obtained during their binding to the sensor surface,[41,42] even at very low surface coverages. In all experiments, the device surface was initially modified through the adsorption of neutravidin (Figure 2, step (i)) followed by the addition of DNA molecules incorporating both a biotin at the 5′-end and a cholesterol at the 3′-end of the same strand (Figure 2, step (ii)) and finally the injection of a solution of liposomes (Figure 2, step (iii)). The neutravidin/biotin methodology for the immobilization was chosen for being both simple and efficient.

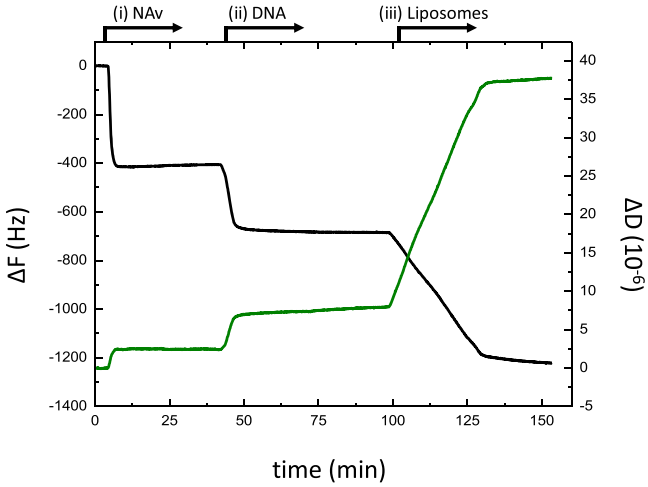

Figure 2. Real-time graph of binding events as recorded at 35 MHz: (i) neutravidin (0.2 mg/mL) is added on the gold surface until saturation, followed by (ii) the binding of biotinylated DNA (here 400 nM of 50 bp) bearing a cholesterol at the other end. The latter can subsequently bind (iii) POPC liposomes (here 0.05 mg/mL of 200 nm). Note that F measurements are used as raw data, i.e., without dividing them with the number of the harmonic.

Measurement of the Dissipation Capacity of DNAs. We started by experimentally calculating the acoustic ratio of three ds DNAs of 21, 50, and 157 bp. The interaction of biotinylated DNA with surface-immobilized neutravidin can be safely considered to be specific because no response is observed with nonbiotinylated DNA (results not shown), leading to single-point DNA attachment. Figure 3 shows that the acoustic ratio of the three dsDNAs is independent of DNA surface coverage following the type (i) curve shown in Figure 1B. As a result, the acoustic ratio of DNA molecules coincides with our definition of the DC value. The observed dependency of the DC value to the DNA length and coverage, with longer DNAs giving higher DC values, is in agreement with previous results from our group.[25,26,36]

Measurement of the Dissipation Capacity of Liposomes. *Calculating ΔD_{Lip} and ΔF_{Lip} at the Plateau.*

https://dx.doi.org/10.1021/acs.analchem.0c00366
Anal. Chem. 2020, 92, 8186−8193

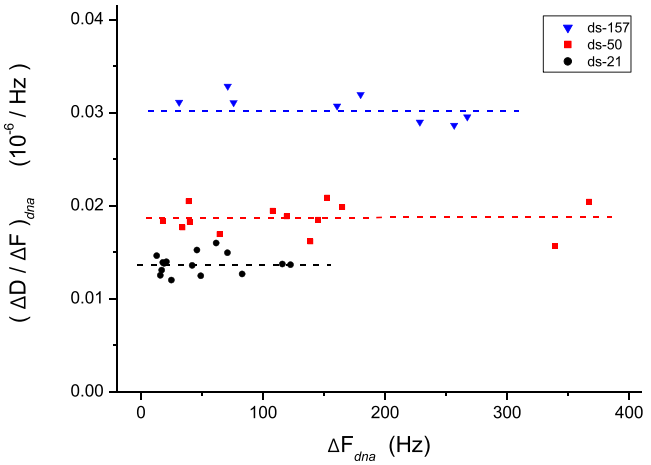

Figure 3. Acoustic ratio of three biotin-labeled dsDNAs of 21, 50, and 157 bp as a function of the corresponding attached amount, measured as $(\Delta F)_{dna}$. Acoustic ratio corresponds to ΔD and ΔF values measured at the plateau of step (ii) of Figure 2 (Figure S1).

Preparations of POPC liposomes of a nominal diameter of 30, 50, 100, and 200 nm were added to the cholesterol-modified surface-bound DNA at various concentrations. Initially, we measured ΔD_{Lip} and ΔF_{Lip} at the plateau of step (iii) shown in Figure 2 (see also Figure S1). These values were used to calculate the acoustic ratio $(\Delta D/\Delta F)_{Lip}$, which was then plotted as a function of the amount of bound particles $(\Delta F)_{Lip}$ (Figure 4). Unlike the bound DNAs, liposomes' acoustic ratio

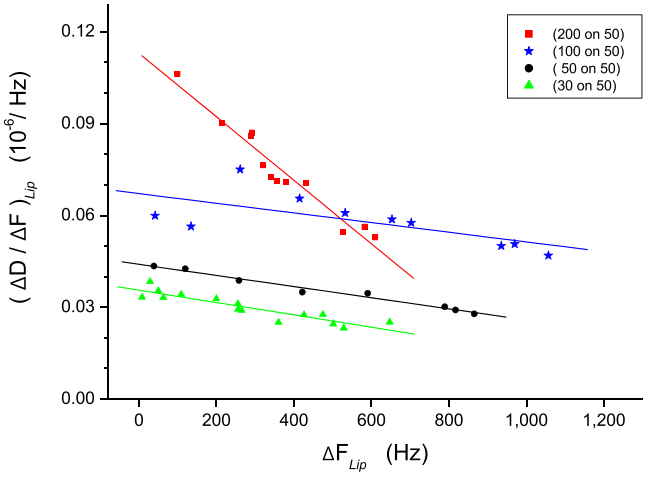

Figure 4. Acoustic ratio of four different POPC liposome sizes (30, 50, 100, and 200 nm) binding to 50 bp DNA. Both ΔD_{Lip} and ΔF_{Lip} were calculated at the plateau of curve (iii) shown in Figure 2.

depends on their surface coverage, something observed in previous studies of surface adsorbed liposomes and other NPs;[21,23,43] interactions between neighboring particles caused by the disruption of the liquid flow at the surface−particle interface was the explanation provided by the authors. We also attribute the $(\Delta D/\Delta F)_{Lip}$ versus ΔF_{Lip} dependency observed in Figure 4 to lateral hydrodynamic cross-talk between neighboring liposomes. However, there are distinct differences between the two systems, i.e., surface-adsorbed and DNA-suspended liposomes. The oscillation of surface-adsorbed liposomes is relatively restricted and more in-phase with the oscillating surface; moreover, the contact area is defined mainly by the bilayer bending modulus and liposome size.[43] Liposomes anchored via DNA exhibit more degrees of freedom and full hydrodynamic coupling with the solvent, leading to a completely different acoustic behavior; this is dictated by both their distance from the surface and the number of DNA anchors per liposome.

Calculating ΔD_{Lip} and ΔF_{Lip} from Real-Time Graphs. To investigate the potential effect of the DNA anchors, we calculated the DC value of liposomes from real-time graphs at $\Delta F_{Lipo} \rightarrow 0$ (Figure S2) and then plotted this value as a function of the DNA coverage ΔF_{dna}. Figure 5A shows that the

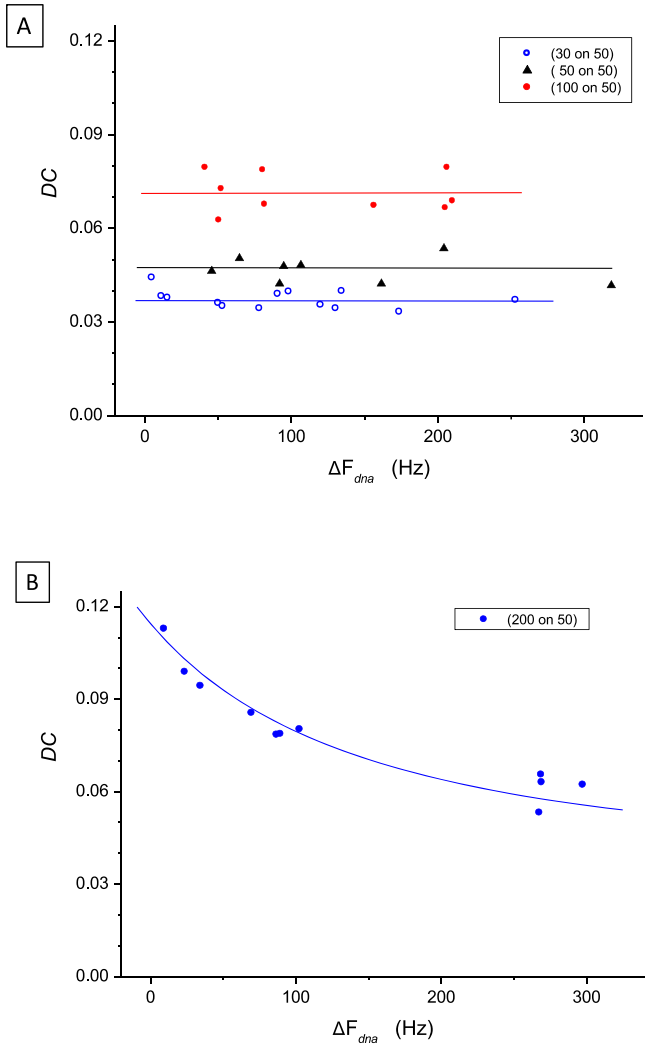

Figure 5. Dependence of the dissipation capacity (DC, 10^{-6}/Hz) of POPC liposomes of (A) 30, 50, and 100 nm and (B) 200 nm anchored to 50 bp DNA as a function of DNA surface coverage ΔF_{dna}. The DC values were derived from real-time graphs (Figure S2).

DC value of smaller liposomes, on average, is not affected by the DNA surface coverage, implying binding through a constant number of anchors. In contrast, liposomes of a diameter of 200 nm show a dependency on the DNA surface coverage (Figure 5B), suggesting multiple anchors. In light of these observations, we conclude that the slope of the $(\Delta D/\Delta F)_{Lip}$ versus ΔF_{Lip} graph observed in Figure 4 reflects the combined effect of lateral interactions and variation in the number of DNA linkers per liposome.

https://dx.doi.org/10.1021/acs.analchem.0c00366
Anal. Chem. 2020, 92, 8186−8193

The intercepts of the lines shown in Figure 5 A and B were calculated and used to derive a value that corresponds to a single liposome bound through a single DNA anchor. These values together with similar values derived for 21 and 157 bp DNA anchors (Figure S3) are summarized in Table 1.

Table 1. Summary of DC Values Obtained for dsDNAs and DNA-Anchored Liposomes of Various Lengths and Diameters, Respectively[a]

#bp	L_{DNA} (nm)	DC (10^{-6} Hz^{-1})	30 nm DC (10^{-6} Hz^{-1})	50 nm DC (10^{-6} Hz^{-1})	100 nm DC (10^{-6} Hz^{-1})	200 nm DC (10^{-6} Hz^{-1})
21	7.1	0.014	0.030	0.041	0.050	0.105
50	17.0	0.018	0.037	0.047	0.071	0.115
157	53.4	0.032	0.057	0.068	0.083	0.134

[a]The latter correspond to a single liposome attached to the surface via a single DNA linker. The value corresponding to the 30 nm liposome attached on a 157 bp dsDNA was calculated theoretically.

Ultrasensitive DNA Detection Using Highly Dissipative Liposome Probes. The DC values presented in Table 1 were derived by adding DNA at concentrations in the nM range (>5 nM); these concentrations were high enough to give a detectable response in both the *D* and *F* signals during DNA binding and represent the limit of direct DNA acoustic detection.[44,45] The next step was to detect very low amounts of DNA, not detectable without liposome amplification. From Table 1, we selected 50 and 200 nm liposomes as signal amplifiers for the detection of various DNA targets (21, 50, 75, and 132 bp) added at a concentration below the detectable nM range.

According to Figure 6A, the dissipation signal can discriminate between different "lollipop" geometries regarding the size of the "head" (i.e., the liposome) but not the length of the "stick" (i.e., the DNA). Moreover, the larger 200 nm liposomes can detect down to 1.2 fmol, or 600 μL of 2 pM dsDNA, while the smaller 50 nm liposomes exhibit a LoD of 10 fmol, or 600 μL of 16 pM dsDNA. According to Figure 6B, the frequency response is the same for all the geometries tested and exhibits an overall lower detection limit (10 fmol or 600 μL of 16 pM) than dissipation. Similar results were obtained with a longer 132 bp DNA, prepared via a 2-step hybridization process (Figure S4).

Potential of Dissipation Sensing To Improve Ultrasensitive DNA Acoustic Detection. In the experiments described earlier, we showed that we can use the DC value of a liposome (or nanoparticle in general) to select a highly dissipative probe for DNA detection through dissipation monitoring. Moreover, we wanted to gain insight into the potential of the methodology to further improve the detection limit by designing more effective dissipation-enhancing probes. The results presented in Table 1 indicate that the sizes of both the dsDNA and liposome in the liposomes/DNA complex

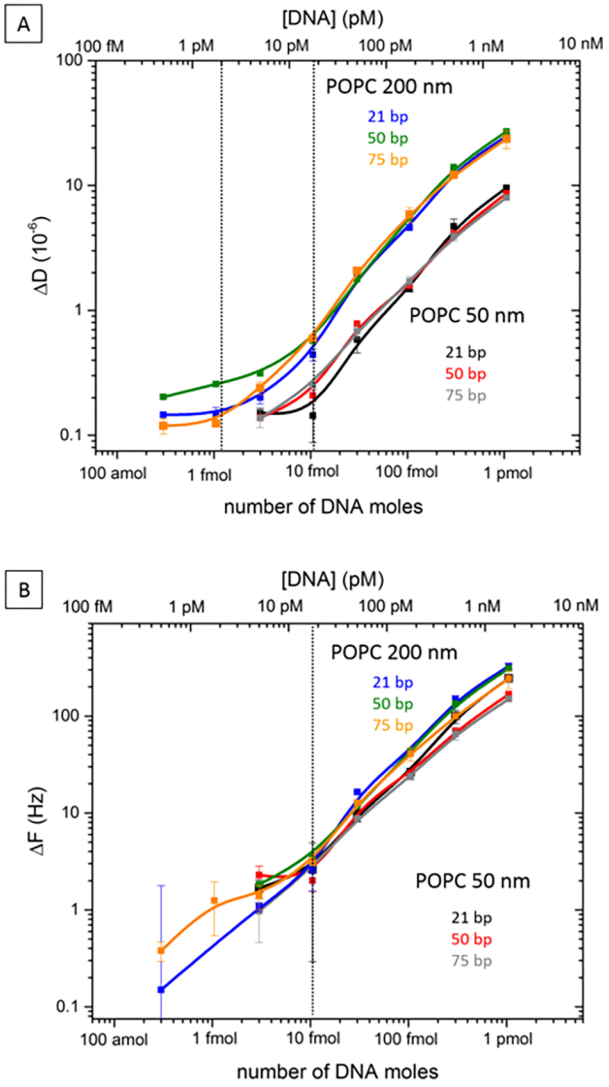

Figure 6. (A) Dissipation and (B) frequency changes obtained during liposome binding to a DNA anchor as a function of the DNA concentration or DNA moles, for three DNA lengths (21, 50, and 75 bp) and two POPC liposome sizes (50 and 200 nm). All points are averages from at least three measurements.

affect the measured DC values; however, for ultrasensitive DNA detection, the DNA length is not significant and the dissipation response is affected primarily by the liposome size (Figure 6A). To derive some guidelines on the correlation between the dissipation capacity of nanoentities and corresponding limit of detection, we plotted the DC values of surface-bound dsDNAs and of DNA/liposome complexes as a function of the number of the DNA base-pairs (Figure 7) on a single graph. Regarding direct dsDNA detection, a DC value of 0.0105 (10^{-6}/Hz) corresponding to 1 bp of DNA (i.e., $\Delta F_{dna} \rightarrow 0$) has a limit of detection in the nM range. Binding on top of the 1 bp DNA a 50 nm liposome with an extrapolated DC value of 0.0370 (10^{-6}/Hz) gives a LoD of 16 pM, while a 200 nm liposome probe with a DC value of 0.1036 (10^{-6}/Hz) brings the LoD further down to 2 pM. Another way to interpret these results is the following: moving from a rigid straight dsDNA (even of 1 bp) to a lollipop-shape structure with a large liposome (200 nm) attached on top of the same DNA results in a ~10 times increase in the DC value and 2500 times decrease in the LoD. This LoD, corresponding to a few

https://dx.doi.org/10.1021/acs.analchem.0c00366
Anal. Chem. 2020, 92, 8186−8193

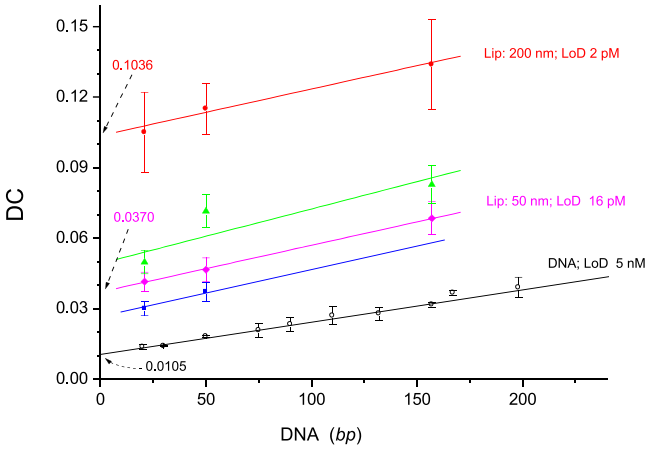

Figure 7. Dependence of the DC value (DC, 10^{-6}/Hz) of DNAs as a function of the DNA length (black line) and of the DC value of POPC liposomes of 30 (blue), 50 (magenta), 100 (green), and 200 (red) nm liposomes attached to dsDNA anchors as a function of the DNA length. The black line is derived experimentally and has been reported in ref 27.

pg of DNA, is 1000 times better than the LoD of classic gel electrophoresis. Overall, Figure 7 suggests that the correlation between DC values and LoD values is affected by the geometry and nature of the attached nanoentity.

Liposomes attached to DNA appear as more promising probes for dissipation signal enhancement than the use of longer dsDNAs (or similar type probes). In this context, trying to increase the POPC liposome size is suggested as a rational strategy for achieving the detection of even lower DNA amounts. In practice, the challenge to design even more dissipative acoustic probes relies on having a better understanding of the exact mechanism of acoustic wave energy dissipation. In this study, we concentrated on the effect of the size of the dsDNA and the DNA/liposome complex on the DC value. Other potential parameters to consider would be the mechanical properties of the liposomes, modulated by the lipids chemical composition and their T_m value; the lipid-bilayer membrane thickness, modulated by the fatty acid length; the surface linker, by using, for example, a suspended neutravidin on surface-bound biotinylated bovine serum albumin (BSA); the use of solid nanoparticles, e.g., silica or gold; and the testing of nonspherical nanoprobe geometries, e.g., ellipsoid, star-shaped, etc. Published results suggest that some of these parameters (e.g., liposomes' shape and stiffness,[40,43] size of colloidal particles,[21,23] and contact stiffness between particles and the surface[22,46]) have an effect on the dissipation. We are currently in the process of evaluating some of these parameters both experimentally and theoretically in order to select optimized dissipative probes of an even higher dissipation capacity.

Application to Molecular Diagnostics. The application of highly dissipative liposomes to molecular diagnostics was investigated in two specific applications. Initially, the ability of 1:1 liposomes−DNA interaction to provide quantitative results when combined with low numbers of PCR amplification cycles was studied. For this purpose, PCR reactions containing samples with the DNA target (positive) and producing 157 bp amplicons modified with biotin and cholesterol at the two 5′ ends were performed in a thermocycler for 5, 10, 15, 20, 25, and 30 cycles (Figure 8A, black line). In addition, PCR reactions with negative samples, i.e., without the target analyte, were also performed for the same number of cycles (Figure 8A, red line).

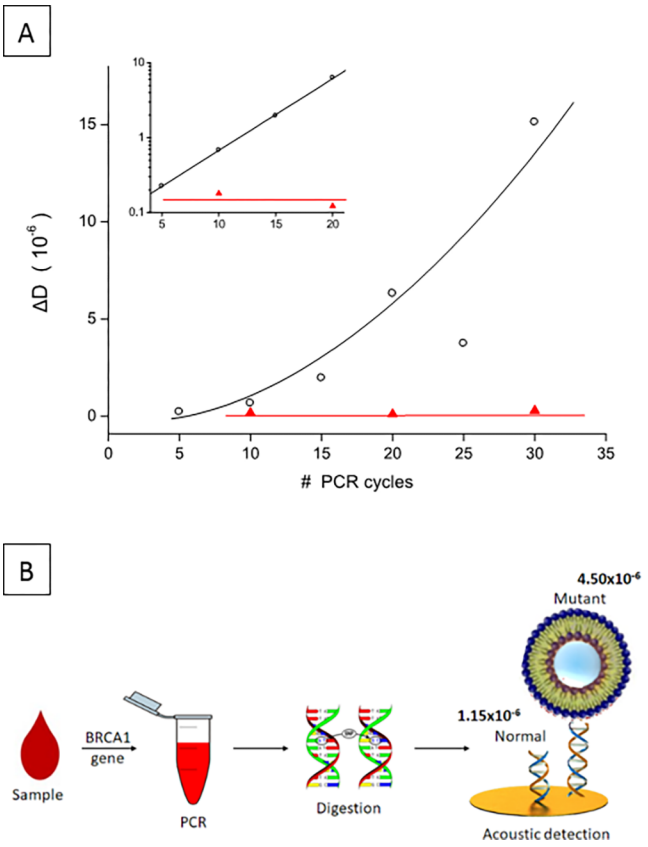

Figure 8. Results related to the use of liposomes as dissipation amplifiers in two real-world molecular diagnostic applications. (A) Change in the dissipation observed during the loading of 200 nm POPC liposomes on DNA produced via PCR as a function of the number of PCR cycles. The black line corresponds to the addition of liposomes on samples containing the target DNA (positive); the red line corresponds to samples without the template (negative). Points belong to a set of experiments, as this is normally carried out to avoid PCR variation. (B) Schematic representation of an assay designed to detect SNP in the $BRCA_1$ gene with the use of 200 nm liposomes.

Double-labeled DNA amplicons employing both a biotin and a cholesterol molecule have been shown to work well upon optimization in both pure and crude samples. Moreover, they offer a versatile means to achieve in a single step surface binding (via biotin) and probe anchoring (via cholesterol), avoiding extra steps for hybridization. After completion of the cycling program, the reactions were loaded without purification on the neutravidin-modified sensor surface followed by the addition of 200 nm liposomes. While the direct binding of the different amounts of DNA produced in each one of these samples could be monitored only after 15 cycles (data not shown), the use of 200 nm liposomes as a dissipation amplifier allowed the reliable detection of amplicons produced after as few as 5 cycles (Figure 8A, inset). A closer look at the data shown in the inset of Figure 8A reveals an exponential increase with excellent correlation ($y = 0.0741\, e^{0.2211x}$, $R^2 = 0.9997$) obtained between 5 and 20 cycles, while the control (addition of liposomes on PCR samples lacking the template, red line in Figure 8A, inset) gave almost zero dissipation. This range of

https://dx.doi.org/10.1021/acs.analchem.0c00366
Anal. Chem. 2020, 92, 8186−8193

cycles does not favor the formation of nonspecific products, which means that reliable quantitative data can be obtained, eliminating the PCR bias response and potential false-positive results. In addition, it was found that as few as 5 pg of human genomic DNA (~1 or 2 target copies) can be used as a template to provide a positive acoustic signal (data not shown). It is worth mentioning that the use of ΔF response for the detection of PCR-amplified DNA after liposome amplification gave much lower sensitivities, with a limit of detection starting from 20 and 15 cycles. These results complement previous studies from our group where liposomes and dissipation-based detection were used during solid-phase isothermal DNA amplification.[47]

In a second example, it was attempted to use dissipative liposomes in a molecular assay designed to achieve single nucleotide polymorphism (SNP) detection in a crude sample such as whole blood. In this case, the unique feature of our methodology to load directly double-stranded DNA and subsequently couple a dissipative probe such as liposomes was exploited for the specific detection of a SNP, i.e., nucleotide base substitution 5331G>A in exon 20 of $BRCA_1$ gene. The presence of a single mutation in $BRCA_1$ is a prognostic/diagnostic biomarker for breast cancer because this mutation exists in 50% of diagnosed cases and forms one of the standard assays performed in a clinical lab. Using 2.5 μL of whole blood, we performed PCR amplification of the target analyte in a total volume of 25 μL. The employed primers were designed to produce 194 bp amplicons with a biotin and a cholesterol on the two opposite 5′ ends. Upon completion of a short cycling process, the reactions were subjected to restriction digestion with the BseRI endonuclease, which digests the normal sequence but not the mutant one. As a result, the immobilized digested amplicons lost the cholesterol-modified end. After completion of the digestion process, the unpurified reactions were loaded on a neutravidin-coated surface followed by the addition of 200 nm liposomes (Figure 8B). The immobilized mutant fragments caused a dissipation signal change of $(4.50 \pm 0.63) \times 10^{-6}$, while the normal fragments resulted in a respective change of $(1.15 \pm 0.43) \times 10^{-6}$, which was attributed to undigested amplicons, a fact verified by gel electrophoresis (data not shown). Still, this was a clear difference that allowed single-base differentiation even in the presence of whole blood and without any purification steps. Additionally, this was a huge improvement compared to the acoustic mutation detection assay described previously, which was based on pure human genomic DNA.[48] This acoustic methodology could also be implemented for other quick genotyping assays for personalized therapies (for example, CYP2C19*2 genotyping for antiplatelet therapy) at the point-of-care.

We should note that, in the described detection setup, we have actually combined the single-copy capabilities of PCR with the enhancing signal capabilities of liposomes to achieve identical LoD to PCR and also quantitative information through dissipation monitoring (Figure 8A). This new method offers two advantages. Because we have reduced the number of PCR cycles, it results in ~33% reduction of the time commonly needed for qPCR. In addition, the method can be employed for detection in the presence of whole blood, which is known to interfere with fluorescence measurements. These are considered the main advantages of our methodology for clinical applications such as screening for mutations or infectious disease testing. Moreover, when compared with next-generation sequencing (NGS), which typically requires the use of a purified DNA template, the exemption in our methodology of DNA extraction makes this method suitable for the development of molecular point-of-care diagnostics such as quick genotyping assays for personalized therapies.

CONCLUSIONS

We designed liposome-decorated dsDNA chains and used the dissipation capacity as a measure to select molecular and particle geometries (DNA length and liposome diameter) that exhibit enhanced acoustic wave energy dissipation. We selected the 200 nm liposomes attached to 21, 50, or 75 bp DNAs for the ultrasensitive detection of 2 pM DNA within a dynamic range covering 3 orders of magnitude, i.e., from nM to pM; this lies well within the clinically relevant concentration range of some biomarkers.[49] Our demonstrated LoD is an improvement of 2.5 times compared to a study also using 200 nm liposomes and a QCM combined with frequency-based measurements.[15] By comparing our methodology to other biosensors employing nanoparticles (normally Au) at a 1:1 target-to-nanoprobe ratio, our performance is similar to detection limits lying in the pM range.[50,51] Substantial improvement occurs when acoustic, electrochemical, or optical systems are combined with multiple nanoprobes[12,19,52] and/or enzymatic amplification.[53−55] However, in addition to improving the LoD in DNA detection assays, an important aspect of this work is the presentation of a new methodology for selecting the most sensitive probe for developing dissipation-monitoring genetic assays. Our results complement other studies,[56] highlighting the particular merits of energy dissipation in biosensing and nanobiotechnology.

ASSOCIATED CONTENT

Supporting Information

The Supporting Information is available free of charge at https://pubs.acs.org/doi/10.1021/acs.analchem.0c00366.

Extra experimental information related to the measurement of the acoustic ratio of DNA and liposomes; dissipation capacity of liposomes anchored on 21 and 157 bp dsDNA; and ultrasensitive detection of 132 bp dsDNA and materials (PDF)

AUTHOR INFORMATION

Corresponding Author

Electra Gizeli − *Institute of Molecular Biology and Biotechnology, Foundation for Research and Technology-Hellas, Heraklion, Crete 70013, Greece; Department of Biology, University of Crete, Heraklion, Crete 71110, Greece;* orcid.org/0000-0002-3598-5984; Email: gizeli@imbb.forth.gr

Authors

Dimitra Milioni − *Institute of Molecular Biology and Biotechnology, Foundation for Research and Technology-Hellas, Heraklion, Crete 70013, Greece*

Pablo Mateos-Gil − *Institute of Molecular Biology and Biotechnology, Foundation for Research and Technology-Hellas, Heraklion, Crete 70013, Greece*

George Papadakis − *Institute of Molecular Biology and Biotechnology, Foundation for Research and Technology-Hellas, Heraklion, Crete 70013, Greece*

https://dx.doi.org/10.1021/acs.analchem.0c00366
Anal. Chem. 2020, 92, 8186−8193

Achilleas Tsortos − *Institute of Molecular Biology and Biotechnology, Foundation for Research and Technology-Hellas, Heraklion, Crete 70013, Greece*
Olga Sarlidou − *Department of Biology, University of Crete, Heraklion, Crete 71110, Greece*

Complete contact information is available at: https://pubs.acs.org/10.1021/acs.analchem.0c00366

Author Contributions

[§]D.M. and P.M.-G. contributed equally.

Notes

The authors declare no competing financial interest.

■ ACKNOWLEDGMENTS

This work was supported by the European Union's Horizon H2020-FETOPEN-1-2016-2017 under Grant agreement no. 737212 (CATCH-U-DNA).

■ REFERENCES

(1) Rosi, N. L.; Mirkin, C. A. *Chem. Rev.* **2005**, *105* (4), 1547−62.
(2) Giljohann, D. A.; Mirkin, C. A. *Nature* **2009**, *462* (7272), 461−4.
(3) Smith, S. J.; Nemr, C. R.; Kelley, S. O. *J. Am. Chem. Soc.* **2017**, *139* (3), 1020−1028.
(4) Saha, K.; Agasti, S. S.; Kim, C.; Li, X.; Rotello, V. M. *Chem. Rev.* **2012**, *112* (5), 2739−79.
(5) Jain, K. K. *Expert Rev. Mol. Diagn.* **2003**, *3* (2), 153−61.
(6) Xu, K.; Huang, J. R.; Ye, Z. Z.; Ying, Y. B.; Li, Y. B. *Sensors* **2009**, *9* (7), 5534−5557.
(7) Zanoli, L. M.; D'Agata, R.; Spoto, G. *Anal. Bioanal. Chem.* **2012**, *402* (5), 1759−71.
(8) Wang, J. *Small* **2005**, *1* (11), 1036−1043.
(9) Antiochia, R.; Bollella, P.; Favero, G.; Mazzei, F. *Int. J. Anal. Chem.* **2016**, *2016*, 2981931.
(10) Merkoci, A. *Biosens. Bioelectron.* **2010**, *26* (4), 1164−77.
(11) Gifford, L. K.; Sendroiu, I. E.; Corn, R. M.; Luptak, A. *J. Am. Chem. Soc.* **2010**, *132* (27), 9265−9267.
(12) D'Agata, R.; Corradini, R.; Ferretti, C.; Zanoli, L.; Gatti, M.; Marchelli, R.; Spoto, G. *Biosens. Bioelectron.* **2010**, *25* (9), 2095−100.
(13) Radwan, S. H.; Azzazy, H. M. *Expert Rev. Mol. Diagn.* **2009**, *9* (5), 511−24.
(14) Hu, K.; Lan, D.; Li, X.; Zhang, S. *Anal. Chem.* **2008**, *80* (23), 9124−30.
(15) Patolsky, F.; Lichtenstein, A.; Willner, I. *J. Am. Chem. Soc.* **2000**, *122* (2), 418−419.
(16) Patolsky, F.; Lichtenstein, A.; Willner, I. *J. Am. Chem. Soc.* **2001**, *123* (22), 5194−205.
(17) Liu, T.; Tang, J.; Jiang, L. *Biochem. Biophys. Res. Commun.* **2002**, *295* (1), 14−6.
(18) Liu, T.; Tang, J.; Jiang, L. *Biochem. Biophys. Res. Commun.* **2004**, *313* (1), 3−7.
(19) Mo, Z. H.; Wei, X. L. *Anal. Bioanal. Chem.* **2006**, *386* (7−8), 2219−2223.
(20) Weizmann, Y.; Patolsky, F.; Willner, I. *Analyst* **2001**, *126* (9), 1502−4.
(21) Olsson, A. L. J.; Quevedo, I. R.; He, D. Q.; Basnet, M.; Tufenkji, N. *ACS Nano* **2013**, *7* (9), 7833−7843.
(22) Peschel, A.; Langhoff, A.; Uhl, E.; Dathathreyan, A.; Haindl, S.; Johannsmann, D.; Reviakine, I. *J. Chem. Phys.* **2016**, *145* (20), 204904.
(23) Tellechea, E.; Johannsmann, D.; Steinmetz, N. F.; Richter, R. P.; Reviakine, I. *Langmuir* **2009**, *25* (9), 5177−5184.
(24) Milioni, D.; Tsortos, A.; Velez, M.; Gizeli, E. *Anal. Chem.* **2017**, *89* (7), 4198−4203.
(25) Tsortos, A.; Papadakis, G.; Gizeli, E. *Biosens. Bioelectron.* **2008**, *24* (4), 836−841.
(26) Tsortos, A.; Papadakis, G.; Mitsakakis, K.; Melzak, K. A.; Gizeli, E. *Biophys. J.* **2008**, *94* (7), 2706−2715.
(27) Tsortos, A.; Papadakis, G.; Gizeli, E. *Anal. Chem.* **2016**, *88* (12), 6472−6478.
(28) Lee, H. S.; Contarino, M.; Umashankara, M.; Schon, A.; Freire, E.; Smith, A. B.; Chaiken, I. M.; Penn, L. S. *Anal. Bioanal. Chem.* **2010**, *396* (3), 1143−1152.
(29) Osypova, A.; Thakar, D.; Dejeu, J.; Bonnet, H.; Van der Heyden, A.; Dubacheva, G. V.; Richter, R. P.; Defrancq, E.; Spinelli, N.; Coche-Guerente, L.; Labbe, P. *Anal. Chem.* **2015**, *87* (15), 7566−7574.
(30) Papadakis, G.; Tsortos, A.; Gizeli, E. *Nano Lett.* **2010**, *10* (12), 5093−5097.
(31) Peh, W. Y. X.; Reimhult, E.; Teh, H. F.; Thomsen, J. S.; Su, X. D. *Biophys. J.* **2007**, *92* (12), 4415−4423.
(32) Mateos-Gil, P.; Tsortos, A.; Velez, M.; Gizeli, E. *Chem. Commun.* **2016**, *52* (39), 6541−6544.
(33) Raptis, V.; Tsortos, A.; Gizeli, E. *Phys. Rev. Appl.* **2019**, *11* (3), 034031.
(34) Johannsmann, D.; Reviakine, I.; Richter, R. P. *Anal. Chem.* **2009**, *81* (19), 8167−8176.
(35) Reviakine, I.; Johannsmann, D.; Richter, R. P. *Anal. Chem.* **2011**, *83* (23), 8838−8848.
(36) Papadakis, G.; Tsortos, A.; Bender, F.; Ferapontova, E. E.; Gizeli, E. *Anal. Chem.* **2012**, *84* (4), 1854−1861.
(37) Johannsmann, D.; Reviakine, I.; Rojas, E.; Gallego, M. *Anal. Chem.* **2008**, *80* (23), 8891−8899.
(38) Patty, P. J.; Frisken, B. J. *Biophys. J.* **2003**, *85*, 996−1004.
(39) Klasczyk, B.; Knecht, V.; Lipowsky, R.; Dimova, R. *Langmuir* **2010**, *26*, 18951−18958.
(40) Melzak, K. A.; Bender, F.; Tsortos, A.; Gizeli, E. *Langmuir* **2008**, *24*, 9172−9180.
(41) Keller, C. A.; Kasemo, B. *Biophys. J.* **1998**, *75* (3), 1397−1402.
(42) Richter, R.; Mukhopadhyay, A.; Brisson, A. *Biophys. J.* **2003**, *85* (5), 3035−3047.
(43) Reviakine, I.; Gallego, M.; Johannsmann, D.; Tellechea, E. *J. Chem. Phys.* **2012**, *136* (8), 084702.
(44) Ferrier, D. C.; Shaver, M. P.; Hands, P. J. W. *Biosens. Bioelectron.* **2015**, *68*, 798−810.
(45) Tang, W.; Wang, D. Z.; Xu, Y.; Li, N.; Liu, F. *Chem. Commun.* **2012**, *48* (53), 6678−6680.
(46) Olsson, A. L. J.; van der Mei, H. C.; Johannsmann, D.; Busscher, H. J.; Sharma, P. K. *Anal. Chem.* **2012**, *84* (10), 4504−4512.
(47) Grammoustianou, A.; Papadakis, G.; Gizeli, E. *IEEE Sens. Lett.* **2017**, *1* (5), 1.
(48) Papadakis, G.; Gizeli, E. *Anal. Methods* **2014**, *6* (2), 363−371.
(49) Kelley, S. O. *Acs Sensors* **2017**, *2* (2), 193−197.
(50) He, L.; Musick, M. D.; Nicewarner, S. R.; Salinas, F. G.; Benkovic, S. J.; Natan, M. J.; Keating, C. D. *J. Am. Chem. Soc.* **2000**, *122* (38), 9071−9077.
(51) Wang, J.; Liu, G. D.; Merkoci, A. *J. Am. Chem. Soc.* **2003**, *125* (11), 3214−3215.
(52) Fang, S. P.; Lee, H. J.; Wark, A. W.; Corn, R. M. *J. Am. Chem. Soc.* **2006**, *128* (43), 14044−14046.
(53) Zhou, W. J.; Chen, Y. L.; Corn, R. M. *Anal. Chem.* **2011**, *83* (10), 3897−3902.
(54) Wan, Y.; Wang, P. J.; Su, Y.; Wang, L. H.; Pan, D.; Aldalbahi, A.; Yang, S. L.; Zuo, X. L. *ACS Appl. Mater. Interfaces* **2015**, *7* (46), 25618−25623.
(55) Lin, M. H.; Wang, J. J.; Zhou, G. B.; Wang, J. B.; Wu, N.; Lu, J. X.; Gao, J. M.; Chen, X. Q.; Shi, J. Y.; Zuo, X. L.; Fan, C. H. *Angew. Chem., Int. Ed.* **2015**, *54* (7), 2151−2155.
(56) Poitras, C.; Tufenkji, N. *Biosens. Bioelectron.* **2009**, *24* (7), 2137−2142.